Journal of Rock Mechanics and Geotechnical Engineering 10 (2018) 91–101

Contents lists available at ScienceDirect

Journal of Rock Mechanics and Geotechnical Engineering

journal homepage: www.rockgeotech.org

Full Length Article

Correlating mode-I fracture toughness and mechanical properties of heat-treated crystalline rocks

Mayukh Talukdar [a], Debanjan Guha Roy [b,*], T.N. Singh [a]

[a] Indian Institute of Technology Bombay, Powai, Mumbai, 400076, India
[b] IITB-Monash Research Academy, Indian Institute of Technology Bombay, Powai, Mumbai, 400076, India

ARTICLE INFO

Article history:
Received 3 May 2017
Received in revised form
17 July 2017
Accepted 6 September 2017
Available online 31 January 2018

Keywords:
Fracture toughness (FT)
Tensile strength (TS)
Ultrasonic velocity
Young's modulus (YM)
Crystalline rocks

ABSTRACT

For the effect of thermal treatment on the mode-I fracture toughness (FT), three crystalline rocks (two basalts and one tonalite) were experimentally investigated. Semi-circular bend specimens of the rocks were prepared following the method suggested by the International Society for Rock Mechanics (ISRM) and were treated at various temperatures ranging from room temperature (25 °C) to 600 °C. Mode-I FT was correlated with tensile strength (TS), ultrasonic velocities, and Young's modulus (YM). Additionally, petrographic and X-ray diffraction analyses were carried out to find the chemical changes resulting from the heat treatment. Further, scanning electron microscopy (SEM) was conducted to observe the micro structural changes when subjected to high temperatures. These experiments demonstrate that heat treatment has a strong negative impact on the FT and mechanical properties of the rocks. From room temperature to 600 °C, mode-I FT values of massive basalt, giant plagioclase basalt, and tonalite were reduced by nearly 52%, 68%, and 64%, respectively. Also, at all temperature levels, FT and mechanical properties are found to be exponentially correlated. However, the exact nature of the relationship mainly depends on rock type. Besides, TS was found to be a better indicator of degradation degree than the mode-I FT. SEM images show that micro crack density and structural disintegration of the mineral grains increase with temperature. These physical changes confirm the observed reduction in the stiffness of heat-treated crystalline rocks.

1. Introduction

Climate change and energy security are the hot topics in the world. Rising economies like China and India are among the biggest consumers of energy in the present era. But concerns regarding the global warming have led to general consensus that greenhouse gas sources such as thermal power plants, cement factories, refineries, and hydrocarbon fuelled transports must be reduced substantially. Therefore, conventional energy must be replaced with renewable energy. In India, coal-based thermal power plant is still the major source of electricity. And the development of multiple renewable energies is the basis of the switch from coal-based power to alternative clean energy sources. Among these clean energy sources, geothermal energy holds a prominent position in India.

India has seven geothermal provinces with various lithological and tectonic settings. Among them, the Deccan Volcanic Province (DVP), which covers 50,000 km^2 of area in central and western India, is particularly interesting. Here, 18 geothermal springs with temperatures varying from 47 °C to 72 °C have already been investigated by Varun et al. (2012). Additionally, peninsular gneiss of South India has recently been identified as a new potential geothermal energy source (Singh et al., 2014). These two areas are shown in Fig. 1.

Development of any geothermal energy project needs an in-depth understanding of the geochemical and mechanical properties of the host rock. Fracture toughness (FT) and mechanical properties are particularly essential for designing the hydraulic fractures in enhanced geothermal systems. Additionally, these properties have tremendous implications in tunnelling, underground excavation, waste disposal site selection, and various problems in reservoir geomechanics. Therefore, it is required to have a good understanding of the effect of ambient geological conditions on FT and mechanical properties of crystalline rocks. One important geological parameter is the subsurface temperature.

* Corresponding author.
E-mail address: geo.debanjan@gmail.com (D. Guha Roy).
Peer review under responsibility of Institute of Rock and Soil Mechanics, Chinese Academy of Sciences.

https://doi.org/10.1016/j.jrmge.2017.09.009

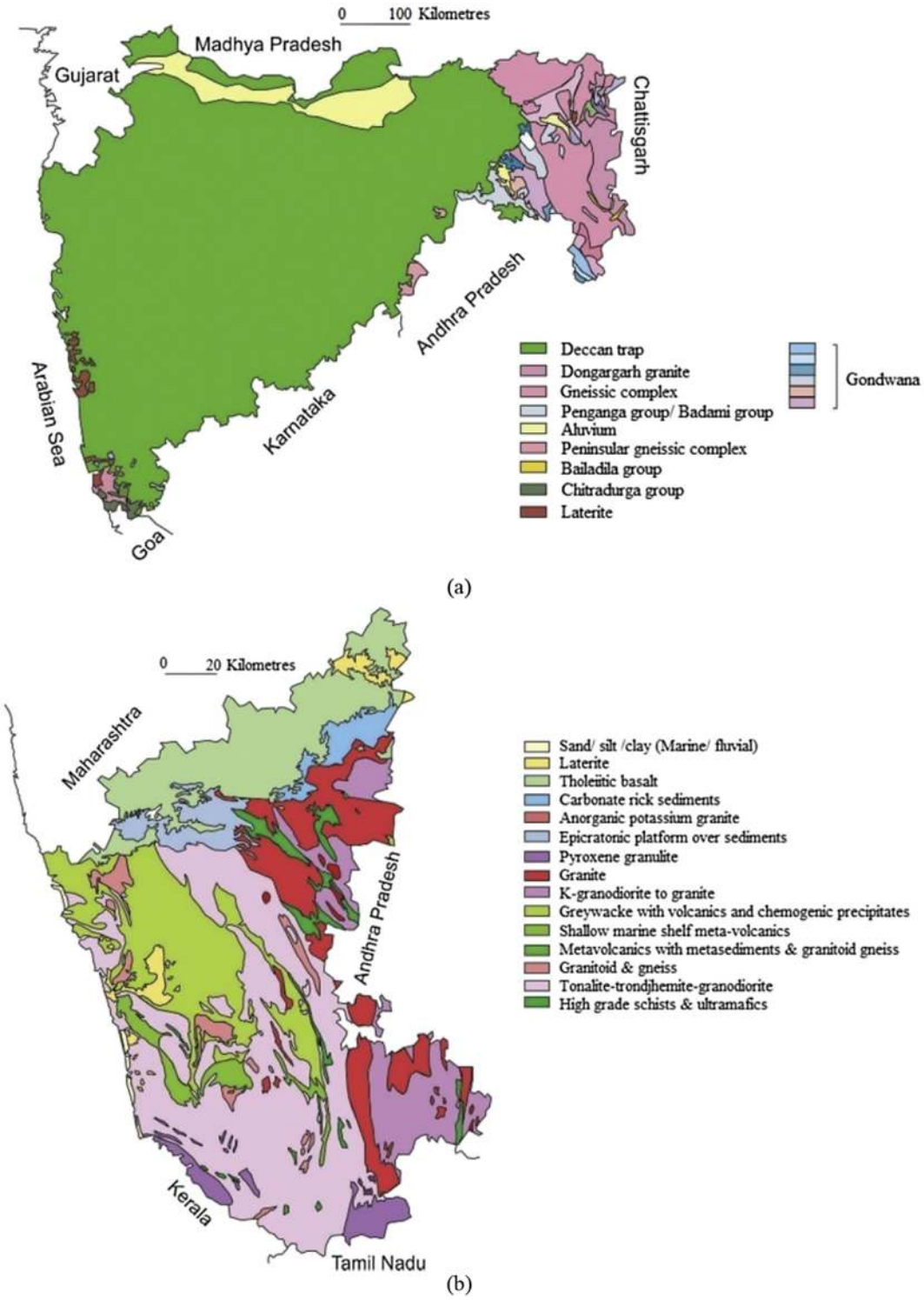

Fig. 1. (a) Geological map of Maharashtra (modified after Geological Survey of India, 2018a), and (b) Geological map of Karnataka (modified after Geological Survey of India, 2018b).

It is well documented that in geothermal systems, temperature can rise up to 200 °C; in underground nuclear disposal sites, temperature varies from 100 °C to 300 °C, if not properly sealed; and in drilling operations down-hole, temperature can be as high as 1000 °C (Paquet and François, 1980; Heuze, 1983; Maheshwar et al., 2015; Shao et al., 2015; Verma et al., 2015; Zhao, 2016).

Several researchers have investigated the temperature-dependent mechanical properties and FT of sedimentary and crystalline rocks (Funatsu et al., 2004, 2014; Nasseri et al., 2007; Kim and Kemeny, 2008; Meier et al., 2009; Vishal et al., 2011; Yin et al., 2012; Ranjith et al., 2012; Liu and Xu, 2014; Guha Roy and Singh, 2016). Meredith and Atkinson (1985) measured the FT

value of the double torsion specimens of Westerly granite and Black gabbro. They reported that in both the rocks, FT increased slightly at the beginning, and then decreased steadily at temperature above 200 °C. Duclos and Paquet (1991) reported a similar decreasing trend of mode-I FT of basalt with increasing temperature. Nasseri et al. (2007) suggested that the FT of Westerly granite decreased by more than 90% from room temperature to 800 °C. Such pattern was also observed by Yin et al. (2015) for Laurentian granite at several loading rates. Investigation on the temperature-dependent strength of crystalline rocks also revealed similar pattern. Bauer and Johnson (1979), Homand-Etienne and Houpert (1989), Dwivedi et al. (2008), and Vishal et al. (2011) conducted experiments on different types of crystalline rocks and they all reported that the strength of rock decreased with increasing ambient temperature. Dwivedi et al. (2008) showed that the tensile strength (TS) of Indian granite decreased by nearly 27% from room temperature to 150 °C, whereas Vishal et al. (2011) reported that TS of khondalite initially increased till 100 °C, and then declined steadily. Similar reduction in Young's modulus (YM) and ultrasonic velocities (P- and S-wave) has also been reported by other researchers for various kinds of rock (Heuze, 1983; Rao et al., 2007; Wu et al., 2013; Zhang et al., 2015).

In spite of great progress made in the laboratory studies concerning the temperature-dependent behaviours of rock properties, major limitations exist in terms of practical and field-scale applications. Sometimes rock cores cannot be retrieved from geothermal wells due to adverse drilling, geological, or economic situations. Even in the cases where rock cores are available, the measurement of FT could be very complex and time-consuming. Additionally, preparation of specimens as per the standard is extremely difficult in fragile and low-strength rocks. Therefore, it is essential to develop indirect prediction method, by which the mechanical properties measured from the traditional well-log data can be used to predict the FT. Past research shows that empirical correlations can be developed between FT and mechanical properties for dry rocks at room temperature (Guha Roy et al., 2017). But no investigation has been done so far to evaluate whether such relationship still exists at elevated temperatures. This issue will be investigated in this work with crystalline rock as a sample.

In this paper, three different types of crystalline rocks, i.e. massive basalt and giant plagioclase basalt (GPB) collected from DVP, as well as tonalite collected from the peninsular gneiss, have been experimentally investigated at temperatures varying from room temperature (25 °C) to 600 °C. The measurement of FT and mechanical properties as per the International Society for Rock Mechanics (ISRM) standards were conducted at each temperature level. This investigation tries to understand the extent of damage, degradation of stiffness, and change in FT value with temperature. Also, the correlation between FT and other mechanical properties have been established to develop prediction models.

2. Laboratory investigation

2.1. Petrography

The petrographic study was conducted under a Leica microscope with representative samples of the rocks prepared into 30 μm thick slides. Minerals were identified based on their optical properties under plane- and cross-polarized light (see Fig. 2). Based on the observations, the mineralogical contents in the specimens were calculated. Results show that GPB consists of plagioclase, pyroxene, olivine, biotite, clay and opaque minerals; tonalite contains plagioclase (Plag), micro-cline (Mic), opaque minerals, biotite (Bt), and muscovite; and massive basalt is composed of plagioclase, pyroxene, biotite, olivine and opaque minerals (OM), in decreasing order. GPB samples have conspicuous euhedral plagioclase laths in

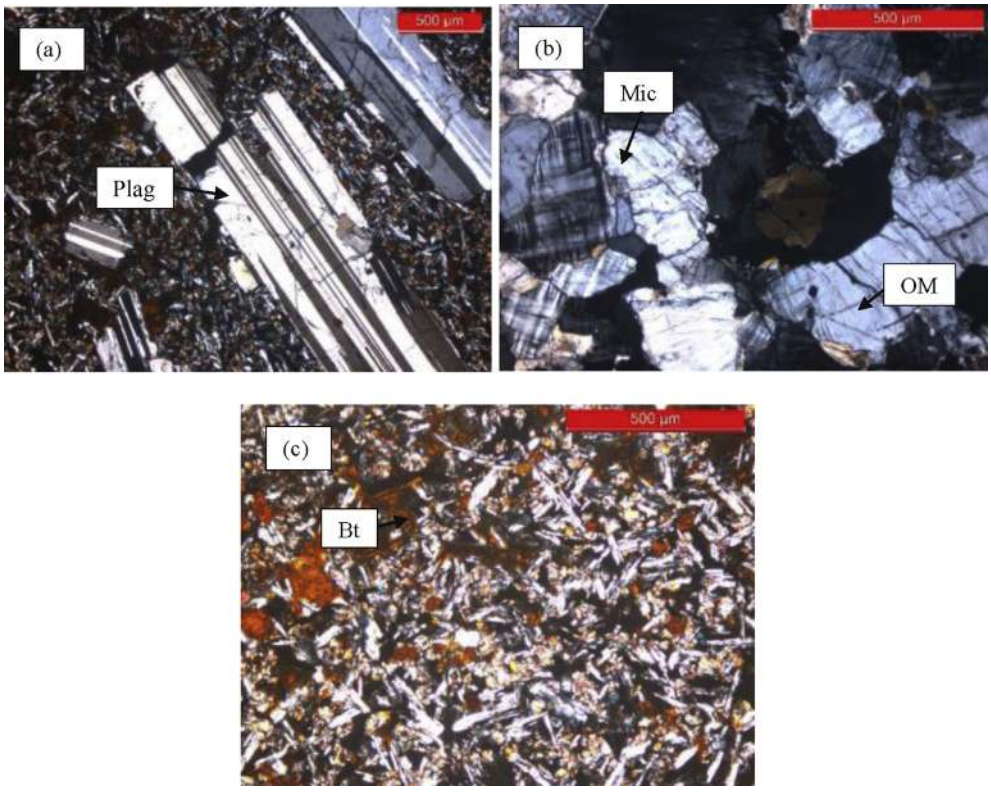

Fig. 2. Micro-graphs of (a) GPB, (b) tonalite, and (c) massive basalt.

a fine-grained groundmass of olivine and pyroxene called porphyritic texture. Tonalite samples are enriched in microcline with formation of triple junctions at the boundaries. Basalt samples are very fine grained where plagioclase laths enclose mainly pyroxene with some traces of olivine, biotite, and opaque.

2.2. Preparation of specimens

The semi-circular bend (SCB) specimens for FT testing were prepared following the ISRM standard (Kuruppu et al., 2014) and are shown in Fig. 3. First, cores were retrieved from the homogenous rock blocks and checked for the damage. Then, undamaged specimens were dried for 72 h. These undamaged specimens were further cut into halves and notched as per dimensions recommended in the standard. Following the recommendations of both ISRM and American Society for Testing and Materials (ASTM), mechanical properties, including TS (ASTM D2845-08, 2008), ultrasonic velocities, and YM (ASTM D3967-08, 2008), were tested. The specimen dimensions used for the experiments are shown in Table 1. The average mechanical properties of the untreated rocks are shown in Table 2. At each temperature level, specimens were treated for 30 d. A constant heating rate of 5 °C/min and cooling rate of 5.3 °C/min were maintained for all the temperature levels. The treated specimens were air-cooled to room temperature for 24 h before testing. Slow rates of heating and cooling help in avoiding thermal shock and making the temperature distribution uniform. For each data point, at least three specimens were tested and the average value was used.

2.3. Mode-I FT calculation

FT represents the resistance of any material against crack propagation. It helps to define the stress distribution in front of a crack tip (Liu, 1983; Kanninen and Popelar, 1985). Therefore, FT is considered as a material property. Many kinds of specimens with different geometries and test configurations have been proposed to correctly calculate different modes of FT, such as cracked chevron notched Brazilian disc (Fowell, 1995; Khan and Al-Shayea, 2000; Chang et al., 2002), short rod specimen (Matsuki et al., 1991), chevron bend specimen (Ouchterlony, 1990), and SCB specimen (Kuruppu et al., 2014). Among them, SCB specimen has been widely used to measure the mode-I FT of different rocks due to its easier specimen preparation, simple instrumental configuration, and convenient experimental set-up (Funatsu et al., 2004, 2014; Ayatollahi and Aliha, 2006; Kuruppu and Chong, 2012; Ayatollahi et al., 2016).

For mode-I FT testing, SCB specimens are prepared with a notch maintaining 0° angle with loading direction. These specimens are then placed in a three-point bend set-up, loaded in a universal testing machine and compressed up to failure. Schematic diagram of the loading unit and a SCB specimen is shown in Fig. 4. A slow and steady displacement rate of 0.2 mm/min was maintained to avoid the effect of impact. The calculation of FT for such specimens is based on the work of Kuruppu et al. (2014). Here, mode-I FT is calculated as

$$K_{IC} = Y' \frac{P_{max}\sqrt{\pi a}}{2RB} \tag{1}$$

where K_{IC} is the fracture toughness, Y' is the dimensionless stress intensity factor, a is the notch length, R is the radius of the specimen, and B is the thickness of the specimen.

For mode-I FT calculation, Y' is calculated as

$$Y' = -1.297 + 9.516\frac{s}{2R} - \left(0.47 + 16.457\frac{s}{2R}\right)\beta + \left(1.071 + 34.401\frac{s}{2R}\right)\beta^2 \tag{2}$$

where $\beta = a/R$ and s is the span between the bottom two rollers.

Fig. 3. Semi-circular bend specimens of (a) massive basalt, (b) giant plagioclase basalt, and (c) tonalite.

Table 1
Geometry specification for the specimens.

Specimen type	Diameter, D (mm)	Thickness, B (mm)	Length, l (mm)	Crack length, a (mm)	Span, s (mm)
SCB specimens	>10 times grain size or = 76	>0.4D or = 30	–	$0.4 \le \frac{a}{R}(\beta) \le 0.6$	$0.5 \le \frac{s}{2R} \le 0.8$
Tensile disc	54.7	38.3	–	–	–
Ultrasonic velocity specimens	54.7	–	110	–	–
Young's modulus specimens	54.7	–	110	–	–

Table 2
Average mechanical properties of untreated rocks.

Rock type	Tensile strength (MPa)	Density (kg/m^3)	P-wave velocity (m/s)	S-wave velocity (m/s)	Young's modulus (GPa)
Massive basalt	24.5	2.91	5978	3803	90.06
GPB	15.29	2.64	5196	3780	71.83
Tonalite	19.36	2.78	5922	3700	80.67

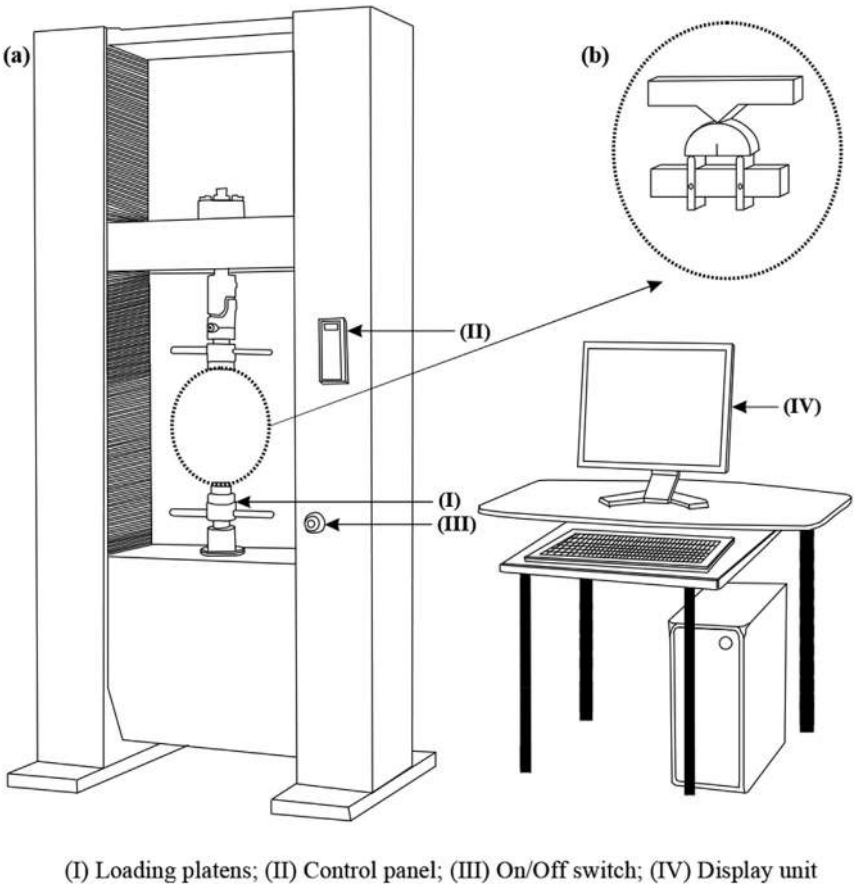

Fig. 4. (a) Universal testing machine and (b) Three-point bend set-up.

3. Results and discussion

3.1. Effect of temperature on FT

Effects of heat treatment on mode-I FT of massive basalt, GPB and tonalite are shown in Fig. 5, where the dimensionless FT has been plotted as a function of the treatment temperature. Here, the dimensionless FT was calculated by dividing the FT at any temperature with the FT at room temperature. The results suggest that the temperature increase has an overall negative effect on FT. Mode-I FT values of GPB and tonalite decreased continuously as temperature increased from room temperature to 200 °C, remained almost constant at temperature between 200 °C and 400 °C–500 °C, and then continued to decrease until temperature up to 600 °C. From room temperature to 200 °C, the FT values of GPB and tonalite decreased by nearly 45% and 64%, respectively, whereas FT values of massive basalt increased by 29%. FT values of massive basalt decreased rapidly at temperature above 200 °C, and the decrease rate was higher at temperature between 200 °C and 400 °C than that between 400 °C and 600 °C. Similar to the present three rocks, degrading values of FT have been reported for gabbro, basalt, and Westerly granite (Meredith and Atkinson, 1985; Duclos and Paquet, 1991). Such decreasing trend indicates that the size of thermal damage zone in rocks is increasing gradually (Balme et al., 2004; Yin et al., 2012). Similar to the behaviour of massive basalt, Meredith and Atkinson (1985), Funatsu et al. (2004), and Rao et al. (2007) also reported an initial increase in toughness till 100 °C–200 °C and a subsequent reduction in higher temperatures. Various researchers have attributed the initial increasing trend to the increase in rock stiffness due to thermal expansion of minerals, and absence of pore water. Balme et al. (2004) explained that thermal expansion of minerals leads to micro crack closure, and this suppression in micro crack linkage causes the increase in toughness. The continuous reduction of toughness in GPB and tonalite and the reduction of toughness in massive basalt above temperature 200 °C are likely due to the development of numerous micro

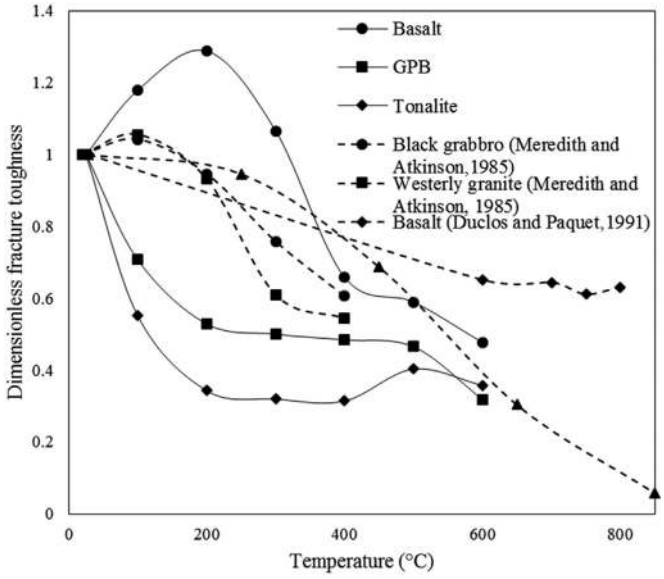

Fig. 5. Change in dimensionless FT with temperature.

cracks throughout the specimens. Increase in treatment temperature causes the development of differential stress at the grain boundaries. And if the differential stress is greater than the TS, new cracks initiate. As explained by Meredith and Atkinson (1985) and Funatsu et al. (2014), generation of a large number of thermal micro cracks reduces the shear resistance and effective stress intensity factor of rocks. As the treatment temperature increases, micro crack density increases and pre-existing cracks become wider. In many cases, these cracks may expand and merge with each other, creating irreversible thermal damage to the material, and leading to a drastic reduction in stiffness (Somerton, 1992; Tian et al., 2012).

3.2. Relationship between FT and TS

TS parameter is one of the most easily determined properties in the laboratory and log analysis. Moreover, both FT and TS indicate resistance against material failure. Previous researches showed that TS was strongly affected by temperature, and most rocks showed an overall decreasing trend (Bauer and Johnson, 1979; Homand-Etienne and Houpert, 1989; Vishal et al., 2011; Liu and Xu, 2014). Also, at room temperature, TS and FT were determined to be strongly linearly correlated with each other (Zhang, 2002; Jin et al., 2011). But no work explores whether such relationship holds true in crystalline rocks at elevated temperatures. In this paper, mode-I FT values of the three rocks have been plotted along with TS in Fig. 6. The results suggest that, FT is exponentially correlated with TS in all the rocks. And the exact trend is strongly controlled by the rock type. The relationships can be expressed as below:

$$\frac{K_{IC}}{K_{IC0}} = 0.4152e^{1.192\frac{\sigma_t}{\sigma_{t0}}} \left(\text{Massive basalt},\ R^2 = 0.68\right) \quad (3)$$

$$\frac{K_{IC}}{K_{IC0}} = 0.1948e^{1.3678\frac{\sigma_t}{\sigma_{t0}}} \left(\text{GPB},\ R^2 = 0.8\right) \quad (4)$$

$$\frac{K_{IC}}{K_{IC0}} = 0.2482e^{1.1211\frac{\sigma_t}{\sigma_{t0}}} \left(\text{Tonalite},\ R^2 = 0.73\right) \quad (5)$$

Subsequently, results from Duclos and Paquet (1991) and Yin et al. (2012, 2015) on glassy basalt and Laurentian granite have also been plotted along with present data for comparison purpose. The plots suggest that both of them confirm the exponential relationship between the mode-I FT and TS at elevated temperatures.

3.3. Relationship between FT and ultrasonic velocities

Dimensionless ultrasonic velocities (P- and S-waves) of the heat-treated specimens as measured by the PUNDIT (portable ultrasonic non-destructive imaging tester) instrument have been plotted along with the dimensionless FT in Fig. 7. Similar to the TS, ultrasonic velocities also maintain exponential relationship with the mode-I FT of crystalline rocks. As the figure suggests, compared to massive basalt, the relationships between FT and P-wave velocity are more obvious in GPB and tonalite. Also, the dispersion of data points suggests that across different temperatures, S-wave velocities vary more than P-wave velocities. The relationships between FT and P-wave velocity of the three crystalline rocks are expressed as below:

$$\frac{K_{IC}}{K_{IC0}} = 0.2521e^{1.5863\frac{V_{pt}}{V_{p0}}} \left(\text{Massive basalt},\ R^2 = 0.6\right) \quad (6)$$

$$\frac{K_{IC}}{K_{IC0}} = 0.0721e^{2.6213\frac{V_{pt}}{V_{p0}}} \left(\text{GPB},\ R^2 = 0.9\right) \quad (7)$$

$$\frac{K_{IC}}{K_{IC0}} = 0.0794e^{2.2887\frac{V_{pt}}{V_{p0}}} \left(\text{Tonalite},\ R^2 = 0.73\right) \quad (8)$$

The relationship between the mode-I FT and S-wave velocity can be expressed as

$$\frac{K_{IC}}{K_{IC0}} = 0.2525e^{1.5\frac{V_{st}}{V_{s0}}} \left(\text{Massive basalt},\ R^2 = 0.73\right) \quad (9)$$

$$\frac{K_{IC}}{K_{IC0}} = 0.1682e^{1.8\frac{V_{st}}{V_{s0}}} \left(\text{GPB},\ R^2 = 0.91\right) \quad (10)$$

$$\frac{K_{IC}}{K_{IC0}} = 0.153e^{1.56\frac{V_{st}}{V_{s0}}} \left(\text{Tonalite},\ R^2 = 0.63\right) \quad (11)$$

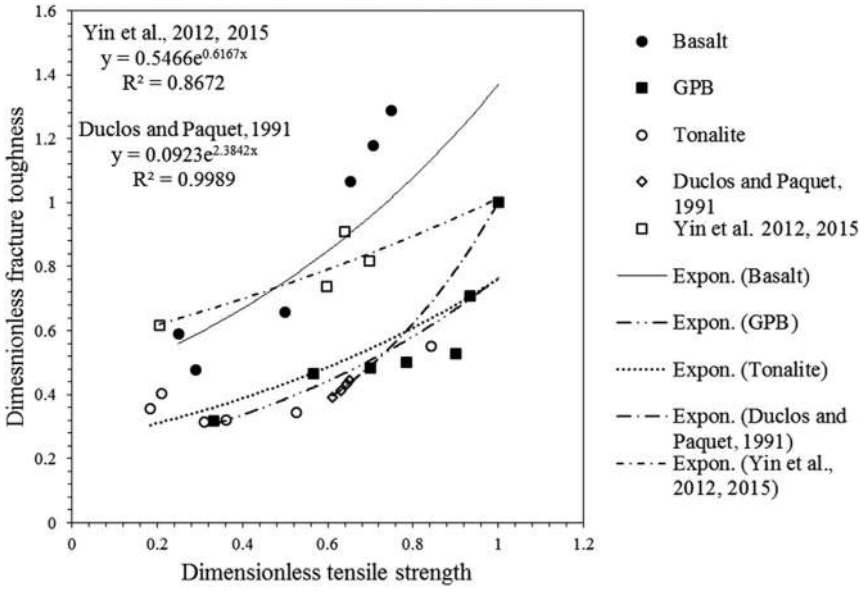

Fig. 6. Relationship between dimensionless FT and dimensionless TS at elevated temperatures.

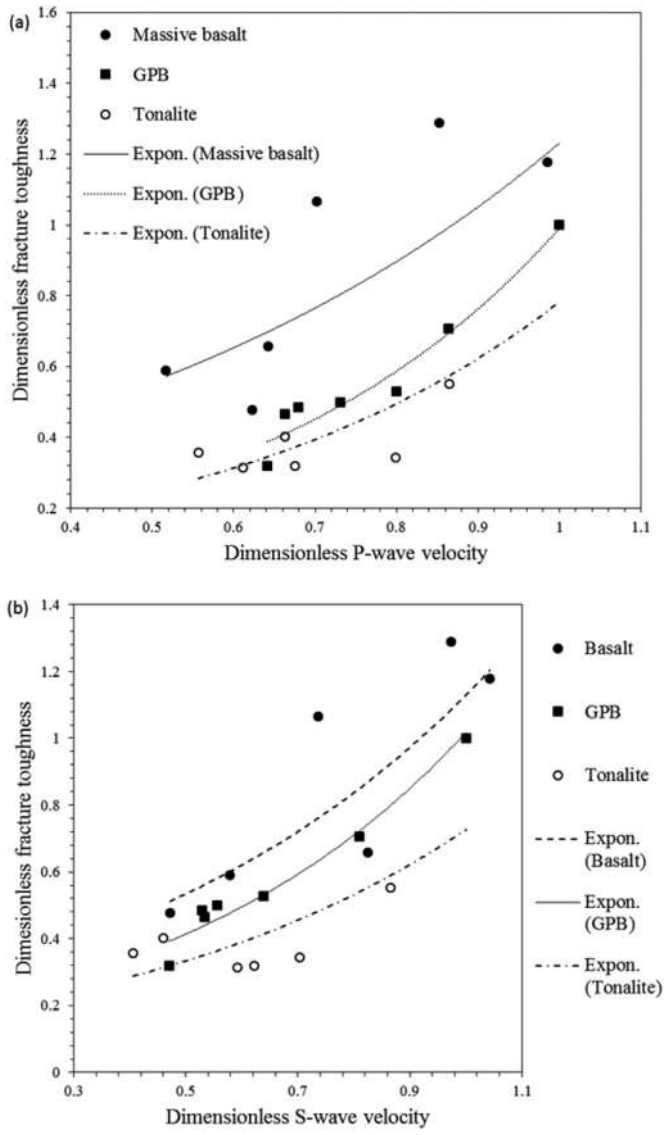

Fig. 7. Dimensionless fracture toughness versus (a) dimensionless P-wave velocity and (b) dimensionless S-wave velocity.

The results suggest that P-wave velocity is more sensitive than S-wave velocity, and can well represent simultaneous changes in mechanical properties. This explained why the relationship between S-wave velocity and FT is less obvious in massive basalt and tonalite.

3.4. Relationship between FT and YM

YM represents the stiffness of a material and the ability to deform under axial stress applied. As discussed previously, thermal damage causes initiation of numerous micro-fractures. With continuous exposure, these cracks expand and merge with each other, reducing the stiffness of the rocks. Therefore, heat-treatment temperature has an immense effect on this parameter. In Fig. 8, the relationship between the mode-I FT and YM of the heat-treated crystalline rocks has been plotted. Across all the temperature levels, these two rock parameters maintain an exponential relationship. Among the three rocks, the relationship in GPB is most obvious, followed by massive basalt and tonalite. The relationships can be expressed as follows:

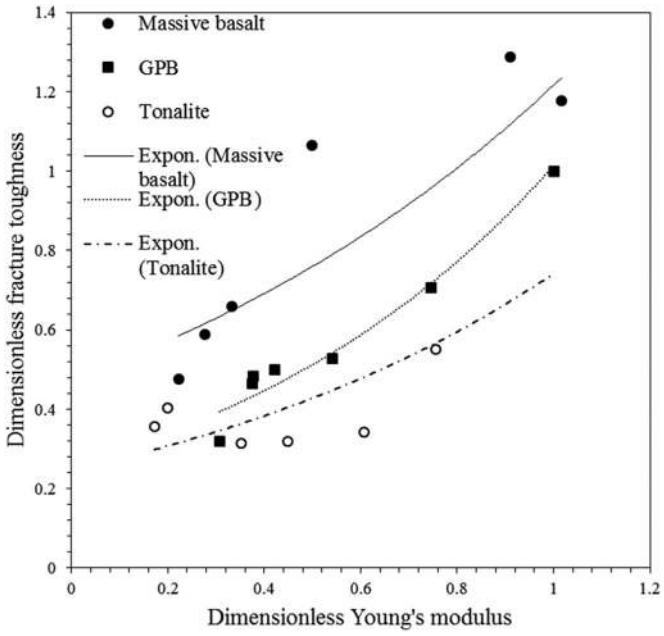

Fig. 8. Relationship between dimensionless FT and dimensionless YM.

$$\frac{K_{IC}}{K_{IC0}} = 0.4746e^{0.9412\frac{YM_t}{YM_0}} \left(\text{Massive basalt},\ R^2 = 0.75\right) \tag{12}$$

$$\frac{K_{IC}}{K_{IC0}} = 0.2589e^{1.3662\frac{YM_t}{YM_0}} \left(\text{GPB},\ R^2 = 0.91\right) \tag{13}$$

$$\frac{K_{IC}}{K_{IC0}} = 0.2468e^{1.1008\frac{YM_t}{YM_0}} \left(\text{Tonalite},\ R^2 = 0.63\right) \tag{14}$$

3.5. Degradation degree (DD)

Thermal damage of any material due to prolonged exposure to high temperature can be expressed as a change in 'degradation degree' (DD). DD indicates the change in the material stiffness and strength. The YM, TS and mode-I FT based on DD have been used in the past to measure the changes in rock strength due to wetting-drying cyclic, freeze-thaw cyclic, and thermal treatment (Li et al., 2012; Jia et al., 2015; Hua et al., 2015, 2016; Gautam et al., 2016). Among them, YM-based method is considered as a standard, and the other two methods have been used sporadically as an attempt to replace it. Here, these three methods are compared to see if TS- and FT-based methods can accurately predict the DD calculated by the YM-based method. These are calculated as

$$D_{YM} = 100\left(1 - \frac{YM_t}{YM_0}\right) \tag{15}$$

$$D_{TS} = 100\left(1 - \frac{\sigma_t}{\sigma_{t0}}\right) \tag{16}$$

$$D_{FT} = 100\left(1 - \frac{K_{ICt}}{K_{IC0}}\right) \tag{17}$$

where D_{YM}, D_{FT} and D_{TS} are the DDs of YM, FT, and TS, respectively; YM_t, σ_t and K_{ICt} are the YM, TS and mode-I FT at a certain temperature, respectively; YM_0, σ_{t0} and K_{IC0} are the YM, TS, and mode-I FT at room temperature, respectively.

The evolution of the DD, as displayed in Fig. 9a, indicates that all the three rocks have undergone continuous but different degrees of degradation when subjected to high temperatures. As explained before, although the GPB and tonalite samples have undergone continuous degradation, massive basalt sample showed an increase in stiffness initially. This behaviour of massive basalt is also reflected in DD calculation by all the methods, albeit to different extents. In all the three methods, there is a drop in DD values for massive basalt from room temperature to 300 °C. While TS and YM have computed low but positive DD values for this temperature range, mode-I FT gave calculated negative values. Fig. 9b shows that, according to the YM-based method, the DD values of massive basalt, GPB, and tonalite are 74%, 69.3%, and 82.7%, respectively, when subjected to temperatures from room temperature to 600 °C. TS-based method made a closer estimate to DD than FT-based method. Therefore, TS can be considered a suitable candidate for DD calculation.

3.6. X-ray diffraction (XRD) and scanning electron microscopy (SEM)

Besides the mechanical properties, chemical composition and rock texture are also affected by high temperature, which is confirmed by XRD analyses of untreated rock and heat-treated rock

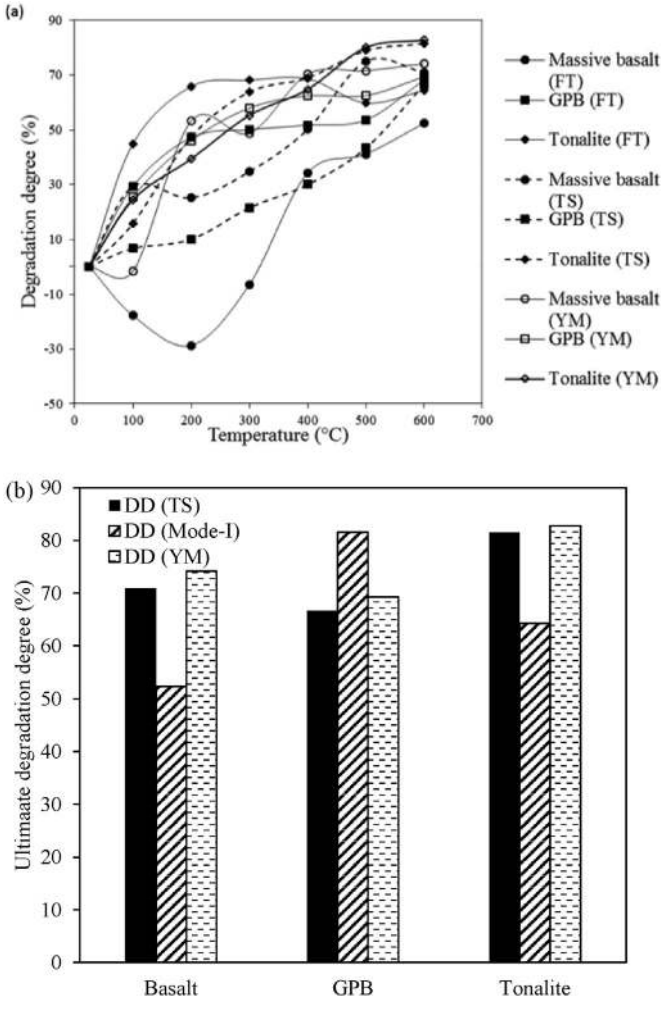

Fig. 9. (a) Evolution of degradation degree with temperature, and (b) Ultimate degradation degree.

(at 600 °C). At temperature of 600 °C, some phases of mica in massive basalt, such as muscovite, phologopite, and biotite, disappeared. Such changes led to higher volumetric fraction of Fe and Ti oxide minerals like magnetite and ilmenite. Similar changes have also been reported by other researchers (Poshusta et al., 1999; Ranjith et al., 2012). Similarly, at high temperature, phyllosilicates and hornblende in tonalite also broke down by releasing the hydroxyl ion. At room temperature, zeolite in tonalite has a chemical formula of $Al_{92}(Cs,Li)_{66}O_{384}Si_{100}$, whereas at 600 °C, zeolite's chemical formula is $H_{0.44}Al_{0.8}Cs_{0.78}Li_{0.02}O_{12.22}Si_{5.2}$, which suggests that zeolite is a good absorbent exposed to hydroxyl ions (Xu et al., 2007). These chemical and mineralogical changes also lead to the changes in the appearance of the minerals and rock grains and textures. SEM images of the untreated and heat-treated rocks are shown in Fig. 10. As shown in Fig. 10a, e and i, the crystalline rock specimens at the room temperature are smooth and crystals are intact, without any holes, inter- or intra-grain cracks. As the treatment temperature is raised to 200 °C, crystal structure remains undisturbed, but surfaces become slightly rough. From 200 °C to 600 °C, numerous cracks appear in the samples, and mineral surfaces become rougher and more irregular. These cracks initially appear at the grain boundaries. At higher temperature, cracking and pulverization of the whole grains are visible. Especially in GPB, intra- and trans-granular cracks are clearly visible at 600 °C. Previous SEM studies of the heat-treated rocks have also revealed the appearance of micro cracks at elevated temperatures (Yin et al., 2012; Zhang et al., 2015). These micro cracks begin at the grain boundaries due to the differential thermal expansion of the adjacent minerals. As the treatment temperature increases, both micro crack density and crack length increase (David et al., 2012; Ranjith et al., 2012). Mahanta et al. (2016) reported highly dense micro cracks in multiple Indian rocks at 500 °C–600 °C. Fig. 10 shows similar observations in the present cases. It is observed that, above 200 °C, massive basalt undergoes more cracking compared to GPB and tonalite, which can explain the steep drop in the mode-I FT of massive basalt above 200 °C. Additionally, the higher FT value of massive basalt compared to GPB and tonalite can also be explained with the generation and propagation of micro cracks. In fine-grained rocks, such as massive basalts, cracks encounter grains frequently, leading to the crack diversion in multiple directions, therefore forming relatively curvilinear or irregular fractures (Wu et al., 1978; Kranz, 1983). This crack pattern maximises the strain energy release rate, which explains the higher FT of massive basalt relative to GPB and tonalite. At temperature of 600 °C, extreme micro cracking, aided by the structural disintegration, can cause pulverization of the minerals. Such changes are the main reasons accounting for the irreversible thermal damage of the rocks.

4. Conclusions

In this context, an attempt has been made to evaluate the temperature-dependent mode-I FT of three crystalline rocks with respect to their relationship with key mechanical properties. Rock specimens were treated at temperatures ranging from room temperature (25 °C) to 600 °C. The key conclusions drawn from this experimental study are:

(1) Temperature has an overall negative effect on the mode-I FT of the rocks, which is strongly controlled by the lithology and grain size.
(2) As the heat-treatment temperature increases, stiffness of the massive basalt increases until temperature up to 200 °C. Beyond 200 °C, a continuous and steep decline is observed. Whereas, both GPB and tonalite display continuous degradation with increasing temperature.

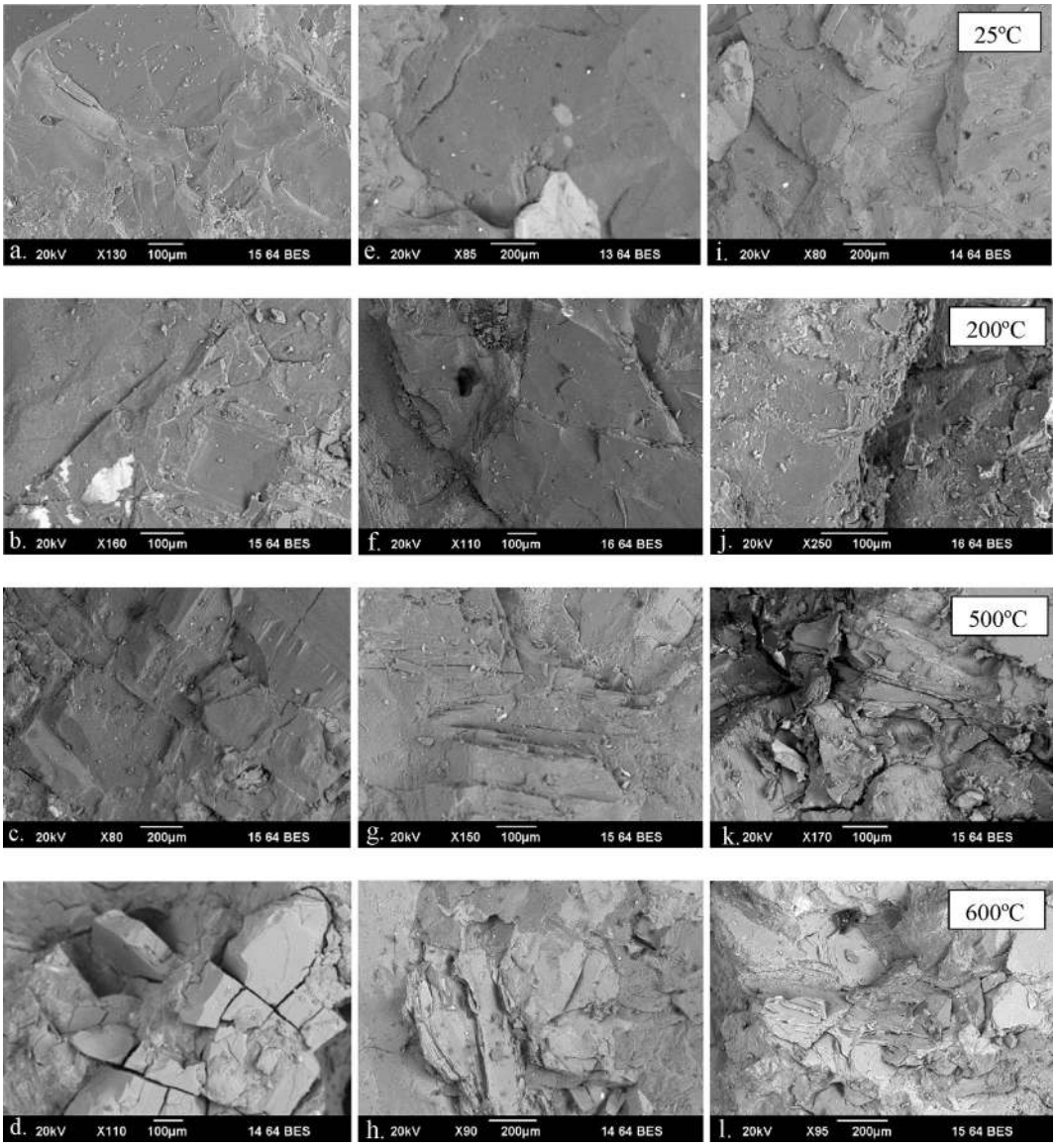

Fig. 10. SEM images of untreated and heat-treated rocks: (a–d) GPB, (e–h) tonalite, and (i–l) massive basalt.

(3) At elevated temperatures, regardless of rock lithology, all key mechanical properties, such as TS, P-wave velocity, S-wave velocity, and YM are exponentially related with FT. Besides, P-wave velocity is a better predictive indicator than the S-wave.
(4) The reduction in stiffness and the extent of thermal damage can be quantified using the 'degradation degree'. Along with the YM, TS is also found to provide reasonably accurate degradation prediction in these three kinds of crystalline rocks.
(5) XRD and SEM studies identify both the chemical and physical changes responsible for the observed changes in FT. At elevated temperatures, water-bearing minerals (i.e. mica) become unstable and break down by releasing the structural water. Such reaction leads to the pulverization of the minerals. In addition, differential thermal expansion of the minerals grains causes the generation and expansion of numerous micro cracks. The increasing micro crack density and pulverization of the minerals are the main two mechanisms accounting for the reduced stiffness and toughness of the rocks.

Conflict of interest

The authors wish to confirm that there are no known conflicts of interest associated with this publication and there has been no significant financial support for this work that could have influenced its outcome.

List of symbols

K_{IC}	Fracture toughness at a certain temperature
K_{IC0}	Fracture toughness at room temperature
Y'	Dimensionless stress intensity factor
a	Notch length
R	Radius of the specimen
B	Thickness of the specimen
s	Span, the distance between the bottom two rollers
σ_t	Tensile strength at a certain temperature
σ_{t0}	Tensile strength at room temperature
V_{pt}	P-wave velocity at a certain temperature
V_{p0}	P-wave velocity at room temperature
V_{st}	S-wave velocity at a certain temperature

V_{s0} S-wave velocity at room temperature
YM_t Young's modulus at a certain temperature
YM_0 Young's modulus at a room temperature
D_{YM} Degradation degree by YM method
D_{FT} Degradation degree by FT method
D_{TS} Degradation degree by TS method

References

ASTM D2845-08. Standard test method for laboratory determination of pulse velocities and ultrasonic elstic constants of rock. West Conshohocken, PA, United States: ASTM International; 2008.

ASTM D3967-08. Standard test method for splitting tensile strength of intact rock core specimens. West Conshohocken, PA, USA: ASTM International; 2008.

Ayatollahi MR, Aliha MRM. On determination of mode II fracture toughness using semi-circular bend specimen. International Journal of Solids and Structures 2006;43(17):5217–27.

Ayatollahi MR, Mahdavi E, Alborzi MJ, Obara Y. Stress intensity factors of semi-circular bend specimens with straight-through and chevron notches. Rock Mechanics and Rock Engineering 2016;49(4):1161–72.

Balme M, Rocchi V, Jones C, Sammonds P, Meredith P, Boon S. Fracture toughness measurements on igneous rocks using a high-pressure, high-temperature rock fracture mechanics cell. Journal of Volcanology and Geothermal Research 2004;132(2–3):159–72.

Bauer SJ, Johnson B. Effects of slow uniform heating on the physical properties of the Westerly and charcoal granites. In: Proceedings of the 20th U.S. Symposium on rock mechanics. Austin, Texas, USA: American Rock Mechanics Association; 1979.

Chang SH, Lee CI, Jeon S. Measurement of rock fracture toughness under modes I and II and mixed-mode conditions by using disc-type specimens. Engineering Geology 2002;66(1–2):79–97.

David EC, Brantut N, Schubnel A, Zimmerman RW. Sliding crack model for nonlinearity and hysteresis in the uniaxial stress–strain curve of rock. International Journal of Rock Mechanics and Mining Sciences 2012;52:9–17.

Duclos R, Paquet J. High-temperature behaviour of basalts – role of temperature and strain rate on compressive strength and KIC toughness of partially glassy basalts at atmospheric pressure. International Journal of Rock Mechanics and Mining Sciences & Geomechanics Abstracts 1991;28(1):71–6.

Dwivedi RD, Goel RK, Prasad VVR, Sinha A. Thermo-mechanical properties of Indian and other granites. International Journal of Rock Mechanics and Mining Sciences 2008;45(3):303–15.

Fowell RJ. Suggested method for determining mode I fracture toughness using cracked chevron notched Brazilian disc (CCNBD) specimens. International Journal of Rock Mechanics and Mining Sciences & Geomechanics Abstracts 1995;32(1):59–64.

Funatsu T, Seto M, Shimada H, Matsui K, Kuruppu M. Combined effects of increasing temperature and confining pressure on the fracture toughness of clay bearing rocks. International Journal of Rock Mechanics and Mining Sciences 2004;41(6):927–38.

Funatsu T, Kuruppu M, Matsui K. Effects of temperature and confining pressure on mixed-mode (I–II) and mode II fracture toughness of Kimachi sandstone. International Journal of Rock Mechanics and Mining Sciences 2014;67:1–8.

Gautam PK, Verma AK, Jha MK, Sarkar K, Singh TN, Bajpai RK. Study of strain rate and thermal damage of Dholpur sandstone at elevated temperature. Rock Mechanics and Rock Engineering 2016;49:3805–15.

Geological Survey of India. Geological map of Maharashtra. accessed on 5th January, 2018a at 02.42 pm. https://employee.gsi.gov.in/cs/groups/public/documents/document/b3zp/mti3/~edisp/dcport1gsigovi127215.gif.

Geological Survey of India. Geological and mineral map of Karnataka & Goa. accessed on 5th January, 2018b at 02.42 pm. https://employee.gsi.gov.in/cs/groups/public/documents/document/b3zp/mti3/~edisp/dcport1gsigovi127202.gif.

Guha Roy D, Singh TN, Kodikara J, Talukdar M. Correlating the mechanical and physical properties with mode-i fracture toughness of rocks. Rock Mechanics and Rock Engineering 2017;50:1941–6.

Guha Roy D, Singh TN. Effect of heat treatment and layer orientation on the tensile strength of a crystalline rock under Brazilian test condition. Rock Mechanics and Rock Engineering 2016;49:1663–77.

Heuze FE. High-temperature mechanical, physical and thermal properties of granitic rocks— a review. International Journal of Rock Mechanics and Mining Sciences & Geomechanics Abstracts 1983;20(1):3–10.

Homand-Etienne F, Houpert R. Thermally induced microcracking in granites: characterization and analysis. International Journal of Rock Mechanics and Mining Sciences & Geomechanics Abstracts 1989;26(2):125–34.

Hua W, Dong S, Li Y, Xu J, Wang Q. The influence of cyclic wetting and drying on the fracture toughness of sandstone. International Journal of Rock Mechanics and Mining Sciences 2015;78:331–5.

Hua W, Dong S, Li Y, Wang Q. Effect of cyclic wetting and drying on the pure mode II fracture toughness of sandstone. Engineering Fracture Mechanics 2016;153:143–50.

Jia H, Xiang W, Krautblatter M. Quantifying rock fatigue and decreasing compressive and tensile strength after repeated freeze-thaw cycles. Permafrost and Periglacial Processes 2015;26(4):368–77.

Jin Y, Yuan J, Chen M, Chen KP, Lu Y, Wang H. Determination of rock fracture toughness K_{IIC} and its relationship with tensile strength. Rock Mechanics and Rock Engineering 2011;44:621.

Kanninen MF, Popelar CH. Advanced fracture mechanics. 1st ed. New York: Oxford Engineering Science Series, Oxford University Press; 1985.

Khan K, Al-Shayea NA. Effect of specimen geometry and testing method on mixed mode i-ii fracture toughness of a limestone rock from Saudi Arabia. Rock Mechanics and Rock Engineering 2000;33(3):179–206.

Kim KM, Kemeny J. Effect of thermal loading on compressional wave velocity, mode i fracture toughness and tensile strength. In: Proceedings of the 42nd US rock mechanics Symposium. San Francisco, California: American Rock Mechanics Association; 2008.

Kranz RL. Microcracks in rocks: a review. Tectonophysics 1983;100(1–3):449–80.

Kuruppu MD, Chong KP. Fracture toughness testing of brittle materials using semi-circular bend (SCB) specimen. Engineering Fracture Mechanics 2012;91:133–50.

Kuruppu MD, Obara Y, Ayatollahi MR, Chong KP, Funatsu T. ISRM-suggested method for determining the mode i static fracture toughness using semi-circular bend specimen. Rock Mechanics and Rock Engineering 2014;47(1):267–74.

Li W, Pour-Ghaz M, Castro J, Weiss J. Water absorption and critical degree of saturation relating to freeze-thaw damage in concrete pavement joints. Journal of Materials in Civil Engineering 2012;24(3):299–307.

Liu H. On the fundamental basis of fracture mechanics. Engineering Fracture Mechanics 1983;17(5):425–38.

Liu S, Xu J. Mechanical properties of Qinling biotite granite after high temperature treatment. International Journal of Rock Mechanics and Mining Sciences 2014;71:188–93.

Mahanta B, Singh TN, Ranjith PG. Influence of thermal treatment on mode I fracture toughness of certain Indian rocks. Engineering Geology 2016;210:103–14.

Maheshwar S, Verma AK, Singh TN, Bajpai RK. Study of thermo-hydro-mechanical processes at a potential site of an Indian nuclear waste repository. Journal of Earth System Science 2015;124(8):1693–708.

Matsuki K, Hasibuan SS, Takahashi H. Specimen size requirements for determining the inherent fracture toughness of rocks according to the ISRM suggested methods. International Journal of Rock Mechanics and Mining Sciences & Geomechanics Abstracts 1991;28(5):365–74.

Meier T, Backers T, Stephansso O. The influence of temperature on mode ii fracture toughness using the punch-through shear with confining pressure experiment. In: Proceedings of Intetnational Symposium on rock mechanics - SINOROCK 2009, the University of Hong Kong. China: International Society for Rock Mechanics; 2009. ISRM-SINOROCK-2009-041.

Meredith PG, Atkinson BK. Fracture toughness and subcritical crack growth during high-temperature tensile deformation of Westerly granite and Black gabbro. Physics of the Earth and Planetary Interiors 1985;39(1):33–51.

Nasseri MHB, Schubnel A, Young RP. Coupled evolutions of fracture toughness and elastic wave velocities at high crack density in thermally treated Westerly granite. International Journal of Rock Mechanics and Mining Sciences 2007;44(4):601–16.

Ouchterlony F. Fracture toughness testing of rock with core based specimens. Engineering Fracture Mechanics 1990;35(1–3):351–66.

Paquet J, François P. Experimental deformation of partially melted granitic rocks at 600–900 °C and 250 MPa confining pressure. Tectonophysics 1980;68(1–2):131–46.

Poshusta JC, Noble RD, Falconer JL. Temperature and pressure effects on CO_2 and CH_4 permeation through MFI zeolite membranes. Journal of Membrane Science 1999;160(1):115–25.

Ranjith PG, Viete DR, Chen BJ, Perera MSA. Transformation plasticity and the effect of temperature on the mechanical behaviour of Hawkesbury sandstone at atmospheric pressure. Engineering Geology 2012;151:120–7.

Rao Q, Wang Z, Xie H, Xie Q. Experimental study of mechanical properties of sandstone at high temperature. Journal of Central South University of Technology 2007;14(Supp. 1):478–83.

Shao S, Ranjith PG, Wasantha PLP, Chen BK. Experimental and numerical studies on the mechanical behaviour of Australian Strathbogie granite at high temperatures: an application to geothermal energy. Geothermics 2015;54:96–108.

Singh HK, Kumar Y, Chandrasekharam D, Gurav T, Singh B. High-heat-producing granites of East Dharwar Craton around Gugi, Karnataka, and their possible influence on the evolution of Rajapur thermal springs, Deccan Volcanic Province, India. Geothermal Energy 2014;2(2). https://doi.org/10.1186/s40517-014-0002-4.

Somerton WH. Thermal properties and temperature-related behavior of rock/fluid systems. 1st ed. Elsevier; 1992.

Tian H, Kempka T, Xu NX, Ziegler M. Physical properties of sandstones after high temperature treatment. Rock Mechanics and Rock Engineering 2012;45:1113–7.

Varun C, Chandrasekharam D, Singh H, Das S. Geologic setting of the Unkeshwar thermal springs, eastern Deccan Volcanic Province, Maharashtra, India. Geothermal Resources Council Transactions 2012;36:799–802.

Verma AK, Gautam P, Singh TN, Bajpai RK. Numerical simulation of high level radioactive waste for disposal in deep underground tunnel. In: Lollino G, Manconi A, Clague J, Shan W, Chiarle M, editors. Engineering Geology for Society and Territory - volume 1: climate change and engineering Geology. Cham: Springer International Publishing; 2015. p. 499–504.

Vishal V, Pradhan SP, Singh TN. Tensile strength of rock under elevated temperatures. Geotechnical and Geological Engineering 2011;29:1127.

Wu CC, Freiman SW, Rice RW, Mecholsky JJ. Microstructural aspects of crack propagation in ceramics. Journal of Materials Science 1978;13(12):2659–70.
Wu G, Wang Y, Swift G, Chen J. Laboratory investigation of the effects of temperature on the mechanical properties of sandstone. Geotechnical and Geological Engineering 2013;31(2):809–16.
Xu R, Pang W, Yu J, Huo Q, Chen J. Chemistry of zeolites and related porous materials: Synthesis and structure. John Wiley & Sons (Asia) Pte Ltd.; 2007.
Yin T, Li X, Cao W, Xia K. Effects of thermal treatment on tensile strength of laurentian granite using Brazilian test. Rock Mechanics and Rock Engineering 2015;48(6):2213–23.
Yin T, Li X, Xia K, Huang S. Effect of thermal treatment on the dynamic fracture toughness of Laurentian granite. Rock Mechanics and Rock Engineering 2012;45(6):1087–94.
Zhang W, Qian H, Sun Q, Chen Y. Experimental study of the effect of high temperature on primary wave velocity and microstructure of limestone. Environmental Earth Sciences 2015;74(7):5739–48.
Zhang ZX. An empirical relation between mode-I fracture toughness and the tensile strength of rock. International Journal of Rock Mechanics and Mining Sciences 2002;39:401–6.
Zhao Z. Thermal Influence on mechanical properties of Granite: a microcracking perspective. Rock Mechanics and Rock Engineering 2016;49(3):747–62.

Mayukh Talukdar gained his MSC degree in Applied Geology from the Department of Earth Sciences, Indian Institute of Technology Bombay, and his BSC degree of Science in Geological Sciences from Jadavpur University. As a part of his MSC thesis work, his research interest was focused on the effect of heat treatment on fracture toughness and mechanical properties of various crystalline rocks from India. Mayukh's interest lies in the field of rock mechanics, geomechanics, energy and earthquakes.